Catalysis Communications 124 (2019) 108–112

Contents lists available at ScienceDirect

Catalysis Communications

journal homepage: www.elsevier.com/locate/catcom

Short communication

# Atmospherical oxidative coupling of amines by UiO-66-$NH_2$ photocatalysis under milder reaction conditions

Ruxue Liu[a], Shuangyan Meng[a], Yali Ma[a], Litong Niu[a], Shuanghong He[a], Xueqing Xu[b], Bitao Su[a], Dedai Lu[a], Zhiwang Yang[a,*], Ziqiang Lei[a,*]

[a] *Key Laboratory of Polymer Materials of Gansu Province , Key Laboratory of Eco-Environment-Related Polymer Materials, Ministry of Education, College of Chemistry and Chemical Engineering, Northwest Normal University, Lanzhou 730070, PR China*
[b] *School of Chemistry and Chemical Engineering, Harbin Institute of Technology, Harbin 150001, PR China*

ARTICLE INFO

*Keywords:*
UiO-66-$NH_2$
Heterogeneous photocatalysis
Amines coupling reaction
Free radicals

ABSTRACT

To assess the mechanism and milder conditions for amines to imines, UiO-66-$NH_2$ was chosen as an efficient photocatalyst for the transformation under light irradiation. A series of experiments for the catching of the active species were performed, and it was proved that holes ($h^+$) and superoxide radicals ($\cdot O_2^-$) were involved when the reaction was performed under air. The reaction also occurred because of the presence of nitrogen-centered radical cations and carbon-centered radicals, which were induced by photogenerated hole ($h^+$) with considerable conversion and selectivity under anaerobic conditions. Our experiments revealed that the catalyst can be recycled for four times.

## 1. Introduction

Semiconductor-based photocatalysis have attracted great interest from researchers for their capacity of environmental remediation and solution of resource shortage [1–3]. Among these studies, heterogeneous catalysis for selective organic transformations under light has attracted great interest from scholars. To date, some selective redox organic transformations in this field have been developed, such as the oxidation of alcohols [4], the reduction of nitroaromatic [5], and the oxidation of toluene [6].

Mostly, imines are formed from amines and aldehyde by condensation; it is always difficult to control the reaction because of the high activity of aldehyde [7]. Heterogeneous photocatalysis seems to be a desirable and green method for the direct conversion of benzylamines into imines [8]. These photocatalysts exhibit excellent catalytic performance under light irradiation but the requirements of concentration of oxygen and temperature are strict. When the mesoporous graphite carbon nitride (mpg-$C_3N_4$) was used as photocatalyst, high oxygen pressure (0.5 MPa) and relative temperature were required [9]. When $WS_2$ was used as a photocatalyst, the yield of the imines decreased significantly because the reaction was performed in the air rather than in $O_2$ [10]. Although core-shell structured CdS@$C_3N_4$ [11] and PCN-222 [12] were used as photocatalysts for this transformation in air, the $O_2$ is still needed as an oxidant. Therefore, it is necessary to assess the reaction to obtain milder conditions and have a better idea of the reaction mechanism.

Metal-organic frameworks (MOFs), a fascinating class of crystal materials because of their special advantages has launched in many fields [13,14] such as gas storage [15], drug delivery [16], and chemical sensors [17]. There also have been reports that MOFs can be applied for the transformation of amines to imines. For example, Garcia et al. reported that MIL-100(Fe) can achieve this transformation but the reaction can occur in the presence of heat [18]. Sun et al. also reported that $NH_2$-MIL-125(Ti) was an efficient photocatalyst for amines to imines [19]. However, oxygen was necessary for the transformation. UiO-66-$NH_2$ is derived from UiO-66 through ligand functionalization for a wider response to the spectrum, owing to its high thermal stability, we choose UiO-66-$NH_2$ as an efficient photocatalyst for the transformation of amines to imines. It can be noted that imines could be detected with considerable conversion whatever under the air or anaerobic condition. Meanwhile, corresponding mechanisms were proposed, as for this situation, the conditions for the conversion of amines to imines is milder and the mechanism is clearer.

## 2. Experimental

UiO-66 and UiO-66-$NH_2$ were synthesized using the same procedure reported previously [20,21]. The detailed experimental procedures are

---

* Corresponding authors.
*E-mail address:* yangzw@nwnu.edu.cn (Z. Yang).

https://doi.org/10.1016/j.catcom.2019.03.011
Received 29 December 2018; Received in revised form 11 March 2019; Accepted 12 March 2019
Available online 14 March 2019

described in the Supporting Information.

## 3. Results and discussion

### 3.1. Characterization

Fig. S1 showed the XRD patterns of pure UiO-66 and UiO-66-$NH_2$. The diffraction peaks of UiO-66 matched well with the calculated ones, providing a clear proof that the sample was synthesized successfully. Further, it was obvious that UiO-66-$NH_2$ and UiO-66 had the same diffraction peaks; this revealed that the functionalization of the organic linker did not affect the crystal structure of UiO-66, which matched previously reported [22]. The morphology of the samples is shown in Fig. S2. The figure showed that there was no obvious difference between UiO-66-$NH_2$ and UiO-66 in morphology.

The FT-IR spectra were also obtained to analyze the structure of UiO-66 and UiO-66-$NH_2$. As shown in Fig. S3, for UiO-66, the peaks that appeared at 1573 $cm^{-1}$ and 1435 $cm^{-1}$ are produced by the asymmetric and symmetric vibrations of carboxyl groups, respectively. The peaks due to the O—H and C—H vibration in the $H_2BDC$ ligand appeared at 819, 769, and 665 $cm^{-1}$, respectively. Compared with UiO-66, for UiO-66-$NH_2$, the two absorption bands detected at 3450 and 3375 $cm^{-1}$ were attributed to the stretching vibrations of N—H, and the peak at 768 $cm^{-1}$ was easily considered as characteristic wagging vibrations of N—H. The stronger band at 1258 $cm^{-1}$ was produced by C—N stretching absorption. The peaks that the asymmetric and symmetric stretching vibrations of C═O appeared at 1655 and 1497 $cm^{-1}$, respectively.

Detailed information of chemical composition and elemental states about UiO-66-$NH_2$ was obtained by XPS. It is demonstrated that Zr, N, C, and O elements were existed in the sample and the results were showed in XPS survey spectrum (Fig. S4a). The high-resolution XPS spectrum of Zr3d indicated that there were two peaks located at around 182.94 eV and 185.30 eV (Fig. S4b), respectively, which belong to $Zr3d_{5/2}$ and $Zr3d_{3/2}$, was indicating the existence of $Zr^{4+}$ [23]. Fig. S4c is the spectrum of N1s, the peak at 399.58 eV was assigned to N species in the $NH_2$ group. Three peaks, located at 288.80 eV, 285.37 eV, and 284.60 eV in the C1s spectrum (Fig. S4d), were attribute to the carbonyl carbon (C═O), carboxylate carbon (O—C═O), and C═C bond of the carbon components in $H_2ATA$ linkers [24]. The O1s spectrum can be deconvoluted into three peaks appeared at 531.02 eV, 531.89 eV, and 532.69 eV (Fig. S4e), respectively. The peak at 532.69 eV was due to the hydroxyl groups, while another two peaks at 531.02 eV and 531.89 eV were the fitted peaks of the Zr—O bonds in UiO-66-$NH_2$ and the carboxylate groups in the $H_2ATA$ linkers [25].

Fig. S5 is the nitrogen adsorption-desorption isotherms of UiO-66 and UiO-66-$NH_2$. The typical IV isotherms show that the two samples bear the mesoporous structure. The BET specific surface area of the as-prepared UiO-66-$NH_2$ is 1030 $m^2 g^{-1}$, although it is less than that of the UiO-66 (1418 $m^2 g^{-1}$) due to the involving of the —$NH_2$ group, it is bigger than that of reported previously (832 $m^2 g^{-1}$) [26]. All the results indicated that UiO-66-$NH_2$ was obtained successfully.

### 3.2. Photo-oxidation coupling of amines

The activity of the as-prepared samples under light illumination was investigated through the photo-oxidation coupling of amines and benzylamine was selected as the model substrate first. To explore the role of -$NH_2$ group on the organic ligand, UiO-66-$NH_2$ and UiO-66 were applied in the reaction under different wavelengths of light. The results are listed in Table 1. When UiO-66-$NH_2$ was used as catalyst, with the illumination of a full spectrum Xenon lamp, the catalytic efficiency of the reaction was much higher than when UiO-66 was used (Table 1, Entry 1). When a Xenon lamp with a 365 nm cut-off filter or a 420 nm cut-off filter was used as the light source, higher conversion was obtained when UiO-66-$NH_2$ was used as photocatalyst than that of UiO-66 (Table 1, Entries 2, 3). All the results indicated that UiO-66-$NH_2$ was a more efficient photocatalyst than UiO-66 for the coupling of amines. The reason is that UiO-66-$NH_2$ shows a wider response to the spectrum by the modification of -$NH_2$ group on the organic ligand. The experimental results are consistent with the UV–vis DRS, which was showed in Fig. S6, Therefore, Xenon lamp with a full spectrum was chosen for the following studies if there was no specific explanation.

**Table 1**
Comparison between UiO-66-$NH_2$ and UiO-66 as catalysts.

| [a]Entry | UiO-66-$NH_2$ | | UiO-66 | |
|---|---|---|---|---|
| | [b]Con. (%) | [c]Sel. (%) | [b]Con. (%) | [c]Sel. (%) |
| 1 | 83 | 99 | 42 | 99 |
| [d]2 | 66 | 99 | 15 | 99 |
| [e]3 | 34 | 99 | 7 | 99 |

a: Catalyst (15 mg), benzylamine (0.1 mmol), reaction time (10*h*); light (Xenon lamp irradiation with the full spectrum), air, 10 h;
b and c: Calculated by GC analysis.
d: Catalyst (15 mg), benzylamine (0.1 mmol), reaction time (10 h); light (Xenon lamp irradiation with a 365 nm cutoff filter), air, 10 h.
e: Catalyst (15 mg), benzylamine (0.1 mmol), reaction time (10 h); light (Xenon lamp irradiation with a 420 nm cut-off filter), air, 10 h.

To obtain the influence of solvents on photocatalytic coupling of benzylamine, the reaction was examined in various solvents. The results are shown in Table 2. It was clear that the solvents affected the results. The adsorption, oxidation, and polarity of solvent are often considered for the factors affecting the process of photocatalytic reaction [27]. For example, polarity affects the condensation reaction process for producing imines. Among the different polar solvents, ethyl acetate, dichloromethane, and DMF have relatively higher polarity, but the lower conversion was obtained (48%, 51%, and 43%, respectively, Table 2, Entries 3, 6, 9). The reason was that competitive adsorption between the solvent and the substrate, which may lead to a slow reaction rate. When reaction was proceeded in toluene and hexane, not only the lower conversion were provided (65% and 36%, respectively, Table 2, Entries 4, 8), but also the inferior selectivity achieved (82% and 87%, respectively, Table 2, Entries 4, 8). Lower conversion but not very high selectivity was appeared when benzotrifluoride was involved in the conversion (Table 2, Entry 5). When acetonitrile, ethanol, and 1,2-dichloroethane were used as the reaction medium (Table 2, Entries 1, 2, 7), the highest conversion and selectivity were obtained when acetonitrile was selected (83% and 99%, respectively, Table 2, Entry 1). Considering all the above results, acetonitrile was chosen as the best medium for the following studies.

To further explore the UiO-66-$NH_2$ as photocatalyst for photocatalytic coupling of amine, a series of amines under light irradiation, the results were listed in Table 3. It showed that benzylamines with electron-donating groups (such as $CH_3$ and $OCH_3$) and electron-

**Table 2**
Photo-oxidation coupling of benzylamine in different solvents.

| [a]Entry | Sol. | [b]Con.% | [c]Sel.% |
|---|---|---|---|
| 1 | acetonitrile | 83 | 99 |
| 2 | ethanol | 81 | 99 |
| 3 | ethyl acetate | 48 | 99 |
| 4 | toluene | 65 | 82 |
| 5 | benzotrifluoride | 71 | 98 |
| 6 | dichloromethane | 51 | 98 |
| 7 | 1,2-dichloroethane | 81 | 99 |
| 8 | hexane | 36 | 87 |
| 9 | DMF | 43 | 86 |

a: Conditions: UiO-66-$NH_2$ (15 mg), benzylamine (0.1 mmol), light, reaction time (10 h);
b and c: Calculated by GC analysis.

**Table 3**
Photo-oxidation coupling of various substituted benzylamine over UiO-66-$NH_2$.

| [a]Entry | Substrate | Product | [b] Conv. (%) | [c] Sele. (%) |
|---|---|---|---|---|
| **1** | 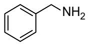 | 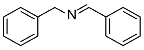 | 83 | 99 |
| **2** | 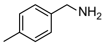 | 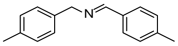 | 52 | 99 |
| **3** | 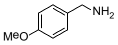 | 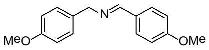 | 58 | 89 |
| **4** | 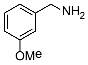 | 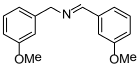 | 43 | 90 |
| **5** | 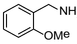 | 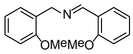 | 29 | 86 |
| **6** | 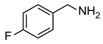 | 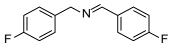 | 68 | 99 |
| **7** | 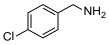 | 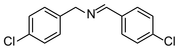 | 44 | 99 |
| **8** | 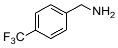 | 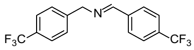 | 43 | 99 |
| **9** | 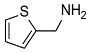 | 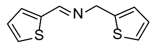 | 83 | 97 |
| **10** | 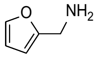 | 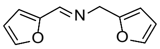 | 99 | 93 |
| **11** | 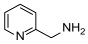 | 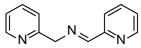 | 40 | 76 |

a: Conditions: UiO-66-$NH_2$ (15 mg), substrate (0.1 mmol), light, reaction time (10 h).
b and c: Calculated by GC analysis.

withdraw groups (such as F, Cl, and $CF_3$) had no definite influence both in the conversion and selectivity (Table 3, Entries 1–8), suggesting that there was no clear electronic effect in this system. Benzylamines with –$OCH_3$ at different position of phenyl ring showed decreased conversion in the order of *orth-* > *meta-* > *para-* position (Table 3, Entries 3–5), indicating that steric hindrance affected this system significantly. Benzylamines with heteroatoms (such as O, S, and N atom), especially heterocyclic amines containing sulfur atoms, which usually considered to be poison agent for most metal catalysts, could also proceed at the same conditions. And it was clearly that the conversion of both thienyl- and furyl- containing methylamine was higher than others.

### 3.3. Photo-oxidation coupling mechanism

To study the possible mechanism of photocatalytic coupling of amines, a series of control experiments were carried out, the results are shown in Table 4. The conversion from starting substrate into final product was very little, which can be negligible when the reaction was performed in dark (Table 4, Entry 5). In the absence of UiO-66-$NH_2$, a similar result was observed (Table 4, Entry 6), suggesting that both light and UiO-66-$NH_2$ were vital for the reaction. Obviously, there was no significant difference in the conversion whether under $O_2$ or air (85% and 83%, respectively, Table 4, Entries 1, 2). Therefore, the condition under air was chosen for the following studies if there was no specific explanation.

To confirm the active species involved in the photocatalytic coupling of amines, *p*-benzoquinone (BQ), as a scavenger of superoxide radical ($\cdot O_2^-$) [28], was added to the reaction system (Table 4, entry 4). The yield of *N*-benzylidene benzylamine decreased significantly to 14%, indicating that $\cdot O_2^-$ is an essential active species in the photo-oxidation coupling of amines. To investigate the role the photoinduced holes ($h^+$) played in the coupling, the reaction was carried out in the presence of KI (Table 4, entry 7), which is known to be the hole scavenger in photocatalytic reactions, the conversions of benzylamine was reduced to 22%, which indicated that $h^+$ was also the vital active species for photocatalytic coupling of amines. These results provided the evidence that $\cdot O_2^-$ and $h^+$ are important in the photocatalytic coupling of amines in the air conditions.

**Table 4**
Active species trapping experiments of the photocatalytic coupling of amines by the catalysis of UiO-66-$NH_2$.

| [a]Entry | Condition. | [b]Con. (%) | [c]Sel. (%) |
|---|---|---|---|
| 1 | $O_2$ | 85 | 99 |
| 2 | Air | 83 | 99 |
| 3 | $N_2$ | 61 | 99 |
| 4 | BQ | 14 | 97 |
| [d]5 | Air | 8 | 99 |
| [e]6 | Air | 11 | 98 |
| 7 | KI | 22 | 99 |
| [f]8 | TEMPO | 3 | 92 |
| [f]9 | KI | 18 | 94 |

a: Conditions: UiO-66-$NH_2$ (15 mg), benzylamine (0.1 mmol), reaction time (10 h).
b and c: Calculated by GC analysis.
d: The reaction was performed in dark.
e: The reaction was performed without UiO-66-$NH_2$.
f: The reaction was performed in the $N_2$.

Based on all the above results, we proposed the possible mechanism for the photocatalytic coupling of amines in the air. As shown in Scheme 1, photoinduced electrons ($e^-$) and $h^+$ were generated when UiO-66-$NH_2$ was illuminated by light, $H_2ATA$ acted as an antenna to

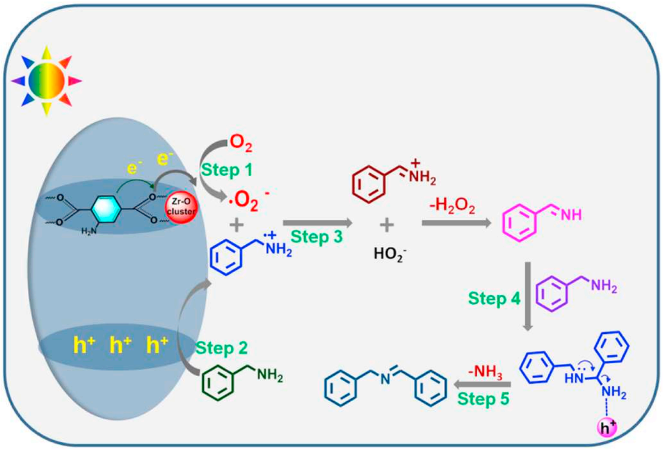

**Scheme 1.** The proposed mechanism for photocatalytic coupling of amine by the UiO-66-$NH_2$ in the air.

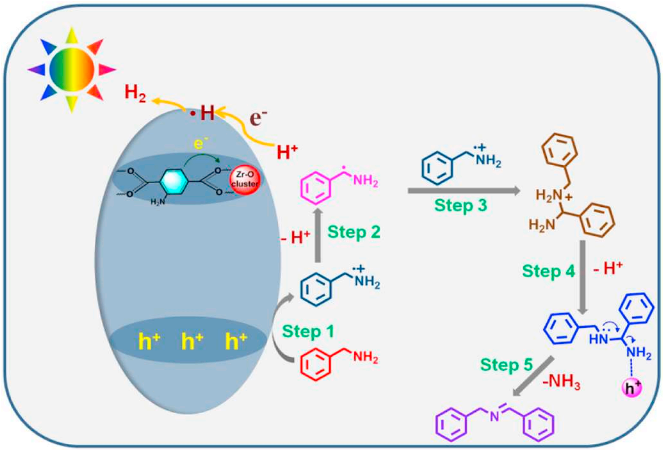

**Scheme 2.** The proposed mechanism for photocatalytic coupling of amine by the UiO-66-$NH_2$ under anaerobic condition.

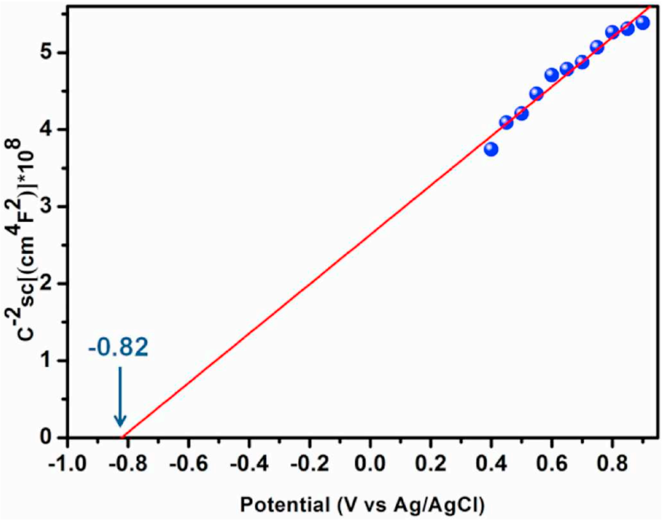

**Fig. 1.** The Mott-Schottky plots of UiO-66-$NH_2$.

absorb light and the energy shifted from $H_2ATA$ to the inorganic zirconium-oxygen clusters [29]. As shown in Fig. 1, the flat-band potential of UiO-66-$NH_2$ was measured using Mott-Schottky plots. It showed that the flat-band potential of UiO-66-$NH_2$ was −0.82 V *vs.* Ag/AgCl (−0.60 V *vs* NHE). The positive slope of the plot revealed an *n*-type semiconductor feature of UiO-66-$NH_2$. For *n*-type semiconductors, the conduction band (CB) position was very close to their flat band potentials [30]. Therefore, the CB of UiO-66-$NH_2$ was −0.60 V (*vs* NHE), which was more negative than the oxidation potential of $O_2/\cdot O_2^-$ (−0.33 V *vs* NHE); thus, the $e^-$ was transformed to $O_2$ to producing one of the main active species of $\cdot O_2^-$, (Step 1 in Scheme 1). Meanwhile, the $h^+$ were transferred to amines, nitrogen-centered radical cations were produced in this process (Step 2 in Scheme 1). Intermediate imine was then generated by the reaction between the $\cdot O_2^-$ and nitrogen-centered radical cations (Step 3 in Scheme 1), which was reactive in the system. These intermediate imines were next attacked by the unreacted amines to generate the next corresponding aminals (Step 4 in Scheme 1). Finally, *N*-benzylidene benzylamines were obtained by hole-assisted elimination of amine group from aminals (Step 5 in Scheme 1).

To investigate the role of $O_2$, further experiments were carried out. Interestingly, the photocatalytic coupling of amines could still be achieved after the removal of $O_2$ from the system by purging with $N_2$ (61%, Table 4, Entry 3). Considering the further research performed by Wang et al. [31], to explain this phenomenon, we speculate that the conversion of benzylamines to the corresponding product was a radical process under the anaerobic conditions. To testify this conclusion, 2,2,6,6-tetramethylpiperidine-1-oxyl (TEMPO), a typical radical scavenger, was added to the reaction system to capture free radicals (Table 4, Entry 8). The yield of the products decreased significantly to about 3%, indicating that free radicals were involved in the reaction. When KI was also added, the conversion of amines decreased to 18% (Table 4, Entry 9). The above results proved that free radicals and $h^+$ were involved in the process. In other words, the presence of free radical and $h^+$ could also promote the transformation.

When the reaction was performed in $N_2$, the proposed reaction mechanism was shown in Scheme 2. Under the light illumination, the $h^+$ was transferred to amines producing nitrogen-centered radical cations (Step 1 in Scheme 2). Then, carbon-centered radicals were generated from nitrogen-centered in a proton transfer (PT) process [32] (Step 2 in Scheme 2). Amino radical cations were then produced through the coupling between nitrogen-centered radical cations and carbon-centered radicals (Step 3 in Scheme 2). With a subsequent PT process to form aminals (Step 4 in Scheme 2). In general, a hole-assisted elimination of amine group occurred in the final process, and *N*-benzylidene benzylamine was formed as the final product (Step 5 in Scheme 2).

### 3.4. Recyclability and stability of the catalyst

The stability of the catalyst was verified by performing the recycle experiments. The catalyst was washed with ethyl alcohol and centrifuged three times after the first run; it was then dried at 100 °C for 12 h, and the recovered catalysts were used in the next run. As shown in Fig. S7a, after four cycles of reuse in the photocatalytic oxidation of benzyl amine, the conversion of benzylamine had no significant decreases and the selectivity of *N*-benzylidene benzylamine was maintained. XRD and FT-IR was used to estimate the structural stability of UiO-66-$NH_2$. As shown in Fig. S7b, the absorption position and the intensity of the peaks of XRD were maintained well after the reaction. This suggested that the crystal structure of UiO-66-$NH_2$ was not destroyed after the recycling. Fig. S7c showed the FT-IR spectra of UiO-66-$NH_2$ after four cycles. No obvious changes were observed. Based on the above results, it is suggested that UiO-66-$NH_2$ possess excellent reusability in the reaction system.

## 4. Conclusions

With the catalysis of the UiO-66-$NH_2$ under light irradiation, the transformation of amines to imines was successfully achieved with considerable conversion and selectivity under air and anaerobic conditions. The possible mechanisms were proposed. The work provides clearer mechanisms for amines to imines and advance a new MOFs based green photocatalysts system for the transformation, Furthermore, it is met the requirements of green chemistry and the sustainable energy development of society. On the other hand, the research also provided the great potential for the application of MOFs-based materials in photocatalytic organic reactions.

## Acknowledgements

The research was financially supported by NSFC (21563026), the Program for Changjiang Scholars and Innovative Research Team in University (IRT15R56), and the Innovation Team Basic Scientific Research Project of Gansu Province (1606RJIA324). We also thank the Key Laboratory of Eco-Environment-Related Polymer Materials (Northwest Normal University), Ministry of Education, and the Gansu International Scientific and Technological Cooperation Base of Water-Retention Chemical Functional Materials, for financial support.

## Appendix A. Supplementary data

Supplementary data to this article can be found online at https://doi.org/10.1016/j.catcom.2019.03.011.

## References

[1] F. Ye, H. Li, H. Yu, S. Chen, X. Quan, Constructing $BiVO_4$-Au@CdS photocatalyst with energic charge-carrier-separation capacity derived from facet induction and Z-scheme bridge for degradation of organic pollutants, Appl. Catal. B Environ. 227 (2018) 258–265.

[2] D. Xu, B. Cheng, W. Wang, C. Jiang, J. Yu, $Ag_2CrO_4$/g-$C_3N_4$/graphene oxide ternary nanocomposite Z-scheme photocatalyst with enhanced $CO_2$ reduction activity, Appl. Catal. B Environ. 231 (2018) 368–380.

[3] Y. Zhang, M. Xu, H. Li, H. Ge, Z. Bian, The enhanced photoreduction of Cr (VI) to Cr (III) using carbon dots coupled $TiO_2$ mesocrystals, Appl. Catal. B Environ. 226 (2017) 213–219.

[4] Z. Yang, X. Xu, X. Liang, C. Lei, Y. Wei, P. He, B. Lv, H. Ma, Z. Lei, MIL-53 (Fe)-graphene nanocomposites: efficient visible-light photocatalysts for the selective oxidation of alcohols, Appl. Catal. B Environ. 198 (2016) 112–123.

[5] Z. Yang, X. Xu, X. Liang, C. Lei, L. Gao, R. Hao, D. Lu, Z. Lei, Fabrication of Ce doped UiO-66/graphene nanocomposites with enhanced visible light driven photoactivity for reduction of nitroaromatic compounds, Appl. Surf. Sci. 420 (2017) 276–285.

[6] S. Samanta, R. Srivastava, Thermal catalysis vs. photocatalysis: a case study with $FeVO_4$/g-$C_3N_4$ nanocomposites for the efficient activation of aromatic and benzylic C-H bonds to oxygenated products, Appl. Catal. B Environ. 218 (2017) 621–636.

[7] S. Zavahir, H. Zhu, Visible light induced green transformation of primary amines to imines using a silicate supported anatase photocatalyst, Molecules 20 (2015) 1941–1954.

[8] X. Lang, H. Ji, C. Chen, W. Ma, J. Zhao, Selective formation of imines by aerobic photocatalytic oxidation of amines on $TiO_2$, Angew. Chem. Int. Ed. 50 (2011) 3934–3937.

[9] F. Su, Smitha C. Mathew, L. Möhlmann, M. Antonietti, X. Wang, S. Blechert, Aerobic oxidative coupling of amines by carbon nitride photocatalysis with visible light, Angew. Chem. Int. Ed. 50 (2011) 657–666.

[10] F. Raza, J. Park, H. Lee, H. Kim, S. Jeon, J. Kim, Visible-light-driven oxidative coupling reactions of amines by photoactive $WS_2$ nanosheets, ACS Catal. 6 (5) (2016) 2754–2759.

[11] Y. Xu, Y. Chen, W. Fu, Visible-light driven oxidative coupling of amines to imines with high selectivity in air over core-shell structured CdS@$C_3N_4$, Appl. Catal. B Environ. 236 (2018) 176–183.

[12] C. Xu, H. Liu, D. Li, J.-H.S.H.- Jiang, Direct evidence of charge separation in a metal–organic framework: efficient and selective photocatalytic oxidative coupling of amines via charge and energy transfer, Chem. Sci. 9 (2018) 3152–3158.

[13] H. Liu, C. Xu, D. Li, H. Jiang, Photocatalytic hydrogen production coupled with selective Benzylamine oxidation over MOF composites, Angew. Chem. 130 (2018) 5477–5481.

[14] J. Xiao, H. Jiang, Metal-organic frameworks for photocatalysis and photothermal catalysis, Acc. Chem. Res. (2018), https://doi.org/10.1021/acs.accounts.8b00521.

[15] A.R. Millward, O.M. Yaghi, Metal-organic frameworks with exceptionally high capacity for storage of carbon dioxide at room temperature, J. Am. Chem. Soc. 127 (2005) 17998–17999.

[16] X. Chen, R. Tong, Z. Shi, B. Yang, H. Liu, S. Ding, X. Wang, Q. Lei, J. Wu, W. Fang, MOF nanoparticles with encapsulated autophagy inhibitor in controlled drug delivery system for antitumor, ACS Appl. Mater. Interfaces. 10 (2018) 2328–2337.

[17] K. Müller-Buschbaum, F. Beuerle, C. Feldmann, MOF based luminescence tuning and chemical/physical sensing, Micropor. Mesopor. Mater. 216 (2015) 171–199.

[18] A. Dhakshinamoorthy, M. Alvaro, Hermenegildo Garcia, Aerobic oxidation of benzyl amines to benzyl imines catalyzed by metal-organic framework solids, ChemCatChem 2 (2010) 1438–1443.

[19] D. Sun, L. Ye, Z. Li, Visible-light-assisted aerobic photocatalytic oxidation of amines to imines over $NH_2$-MIL-125(Ti), Appl. Catal. B Environ. 164 (2015) 428–432.

[20] R. Wang, L. Gu, J. Zhou, X. Liu, F. Teng, C. Li, Y. Shen, Y. Yuan, Quasi-polymeric metal-organic framework UiO-66/g-$C_3N_4$ heterojunctions for enhanced photocatalytic hydrogen evolution under visible light irradiation, Adv. Mater. Interfaces 2 (2015) 1500037.

[21] L. Shen, W. Wu, R. Liang, R. Lin, L. Wu, Highly dispersed palladium nanoparticles anchored on UiO-66($NH_2$) metal-organic framework as a reusable and dual functional visible-light-driven photocatalyst, Nanoscale 5 (2013) 9374–9382.

[22] L. Shen, S. Liang, W. Wu, R. Liang, L. Wu, Multifunctional $NH_2$-mediated zirconium metal-rganic framework as an efficient visible-light-driven photocatalyst for selective oxidation of alcohols and reduction of aqueous Cr(VI), Dalton Trans. 42 (2013) 13649–13657.

[23] L. Shen, S. Liang, W. Wu, R. Liang, L. Wu, CdS-decorated UiO–66 ($NH_2$) nanocomposites fabricated by a facile photodeposition process: an efficient and stable visible-light-driven photocatalyst for selective oxidation of alcohols, J. Mater. Chem. A 1 (2013) 11473–11482.

[24] Y. Su, Z. Zhang, H. Liu, Y. Wang, $Cd_{0.2}Zn_{0.8}S$@UiO-66-$NH_2$ nanocomposites as efficient and stable visible-light-driven photocatalyst for $H_2$ evolution and $CO_2$ reduction, Appl. Catal. B Environ. 200 (2017) 448–457.

[25] X. Xu, R. Liu, Y. Cui, X. Liang, C. Lei, S. Meng, Y. Ma, Z. Lei, Z. Yang, PANI/FeUiO-66 nanohybrids with enhanced visible-light promoted photocatalytic activity for the selectively aerobic oxidation of aromatic alcohols, Appl. Catal. B Environ. 210 (2017) 484–494.

[26] Z. Sha, J. Sun, H. Sze On Chan, S. Jaenicke, J. Wu, Bismuth tungstate incorporated zirconium metal-organic framework composite with enhanced visible-light photocatalytic performance, RSC Adv. 4 (2014) 64977–64984.

[27] S. Samanta, S. Khilari, R. Srivastava, Stimulating the visible-light catalytic activity of $Bi_2MoO_6$ nanoplates by embedding carbon dots for the efficient oxidation, cascade reaction, and photoelectrochemical $O_2$ evolution, ACS Appl. Nano Mater. 1 (2017) 426–441.

[28] Z. Wang, X. Lang, Visible light photocatalysis of dye-sensitized $TiO_2$: the selective aerobic oxidation of amines to imines, Appl. Catal. B Environ. 224 (2018) 404–409.

[29] D. Sun, Y. Fu, W. Liu, L. Ye, D. Wang, L. Yang, X. Fu, Z. Li, Studies on photocatalytic $CO_2$ reduction over $NH_2$-Uio-66(Zr) and its derivatives: towards a better understanding of photocatalysis on metal organic frameworks, Chem. Eur. J. 19 (2013) 14279–14285.

[30] R. Liang, L. Shen, F. Jing, W. Wu, N. Qin, R. Lin, L. Wu, $NH_2$-mediated indium metal-organic framework as a novel visible-light-driven photocatalyst for reduction of the aqueous Cr(VI), Appl. Catal. B Environ. 162 (2015) 245–251.

[31] M. Wang, L. Li, J. Lu, N. Luo, X. Zhang, F. Wang, Photocatalytic coupling of amines to imidazoles using Mo-$ZnIn_2S_4$ catalyst, Green Chem. 19 (2017) 5172–5177.

[32] L. Ye, Z. Li, $ZnIn_2S_4$: a photocatalyst for the selective aerobic oxidation of amines to imines under visible light, ChemCatChem 6 (2014) 2540–2543.